ELSEVIER

Journal of Power Sources 97–98 (2001) 525–528

JOURNAL OF POWER SOURCES

www.elsevier.com/locate/jpowsour

On the correlation between the electroanalytical behavior and crystallographic features of Li-intercalation electrodes

M.D. Levi[a], E. Levi[a], D. Aurbach[a,*], M. Schmidt[b], R. Oesten[b], U. Heider[b]

[a]*Department of Chemistry, Bar-Ilan University, Ramat-Gan 52900, Israel*
[b]*Merck KGaA, 250 Frankfurter Str., Darmstadt, Germany*

Received 23 June 2000; accepted 5 January 2001

Abstract

The electroanalytical behavior of Li_xNiO_2 and $Li_xCo_{0.2}Ni_{0.8}O_2$ was studied by simultaneous application of slow-scan rate cyclic voltammetry (SSCV), potentiostatic and galvanostatic intermittent titration (PITT and GITT), and electrochemical impedance spectroscopy (EIS). Application of a finite-space diffusion model for treating the results obtained by these techniques allowed us to calculate the diffusion coefficient of Li ions (D) and the differential (incremental) capacity (C_{int}) as functions of the electrode's potential. Our final purpose was to compare D versus E and C_{int} versus E plots for both the electrodes, in order to correlate the observed difference in their electroanalytical behavior with the clear distinction in the related Li-insertion mechanisms deduced from XRD studies. While Li insertion into $Li_xCo_{0.2}Ni_{0.8}O_2$ exhibits a single-phase reaction upon charge in the 3.0–4.08 V (versus Li/Li^+) range, Li intercalation into Li_xNiO_2 undergoes two-phase transitions in the same potential range. The shape of both plots, D versus E and C_{int} versus E for these electrodes, is discussed in the framework of a finite-space diffusion model and Li-insertion processes that can be described by Frumkin-type intercalation isotherms with short-range attraction interactions among intercalation sites.

Keywords: Lithium rechargeable batteries; Li_xNiO_2 and $Li_xCo_{0.2}Ni_{0.8}O_2$ electrodes; Impedance spectroscopy; Chemical diffusion coefficient of Li-ions

1. Introduction

Recently, we have reported on the electroanalytical behavior of thin composite Li_xMO_y electrodes studied by simultaneous application of slow-scan rate cyclic voltammetry (SSCV), potentiostatic intermittent titration (PITT), and electrochemical impedance spectroscopy (EIS) [1–4]. The benefit of the simultaneous application of the different electroanalytical techniques is as follows: from the electrochemical point of view, the cathodes for Li-ion batteries under study are not well defined systems. They are usually composite electrodes containing, in addition to their active mass, a polymeric binder (e.g. poly vinylidene difluoride, PVdF), and an electrically conductive additive (carbon black, graphite, etc.), whereas most of the theoretical approaches are applicable to strictly homogeneous thin film electrodes. Application of different techniques with overlapping characteristic time-windows increases the reliability of the various calculated parameters for the Li-ion intercalation, such as D and C_{int} (versus E).

The main objective of this paper was to show how the peak-shaped D versus E and C_{int} versus E plots, experimentally obtained for Li_xNiO_2 and $Li_xCo_{0.2}Ni_{0.8}O_2$ electrodes, correlate with their structural changes during Li-intercalation, and can be described as insertion processes with Frumkin-type intercalation isotherms in which short-range attractive interactions between the intercalation sites determine the Li-intercalation mechanism.

2. Experimental

Li_xMO_y (M = Co, Ni, Mn) powders were obtained from Merck (0.5–1 μm average particle size). The electrode's active mass was 85 wt.% of the corresponding oxide, 10 wt.% conductive carbon black, and 5 wt.% PVdF binder. The three-electrode cell contained a polyethylene frame with symmetrical slits on both sides. The frame holds the working and counter electrodes in a parallel plate configuration with Li counter and reference electrodes. The electrolyte solution was 1 M $LiAsF_6$ (Lithco) in an ethylene carbonate (EC) + dimethyl carbonate (DMC) 1:3 mixture (Merck ultrapure solvents). The electrochemical instrumentation for the PITT and SSCV measurements included a

* Corresponding author. Tel.: +972-3-5326309; fax: +972-3-5351250.
E-mail address: aurbach@mail.biu.ac.il (D. Aurbach).

0378-7753/01/$ – see front matter
PII: S0378-7753(01)00667-X

Schlumberger 1286 electrochemical interface driven by the Corrware software from Scribner Assoc. (Pentium IBM PC). In the vicinity of the differential capacity peaks, the incremental potential steps in the PITT experiments were as small as 10 mV (in a few experiments, the step height was reduced to 5 mV). Each subsequent step was applied after complete equilibration during the proceeding step. Residual (background) currents were less than 0.5 μA/mg.

3. Results and discussion

Figs. 1 and 2 show two highly resolved plots of the differential intercalation capacity, C_{int}, and the chemical diffusion coefficient of the Li-ions, D, versus potential for Li_xNiO_2 and $Li_xCo_{0.2}Ni_{0.8}O_2$ electrodes, respectively. The differential intercalation capacity was obtained from a slow-scan rate cyclic voltammetric curve: $C_{\text{int}}(E) = I(E)v^{-1}$, $v = 10$ μV/s. Li-solid state diffusion was treated here for the simplest case of one-dimensional solid-state diffusion, according to which D is inversely proportional to the diffusion time constant τ:

$$D = \frac{l^2}{\tau} \tag{1}$$

with l denoting the characteristic diffusion length. Here, we identify l with half of the average particle size ($l = 0.5$ μm). The diffusion time constant τ is defined by the following equation [4,5]:

$$\tau = \left[\frac{Q_{\text{m}}\,\Delta X}{\pi^{1/2} I t^{1/2}}\right]^2 = \left[\frac{Q_{\text{m}}(\Delta X/\Delta E)}{\pi^{1/2} I t^{1/2}/\Delta E}\right]^2 = \left[\frac{C_{\text{int}}}{\pi^{1/2} I t^{1/2}/\Delta E}\right]^2 \quad \text{at } t \ll \tau, \tag{2}$$

where Q_{m} denotes the total intercalation charge of the electrode, $X(E)$ is the intercalation level (and hence, ΔX is the change in X during a specific potential step), and $It^{1/2}$ is the Cottrell slope obtained from the linear portion of the I versus $t^{1/2}$ curve for each potential step.

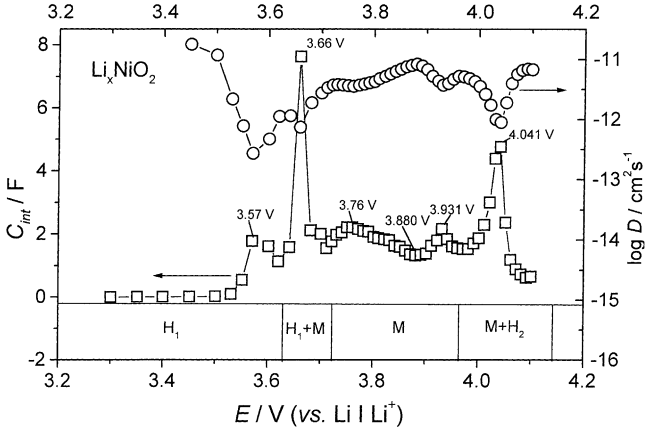

Fig. 1. Plots of the differential intercalation capacity, C_{int} ($v = 10$ μV/s) and the chemical diffusion coefficient of Li-ions, D vs. potential for Li_xNiO_2. The phase diagram of this electrode, shown at the bottom, was obtained by XRD [6].

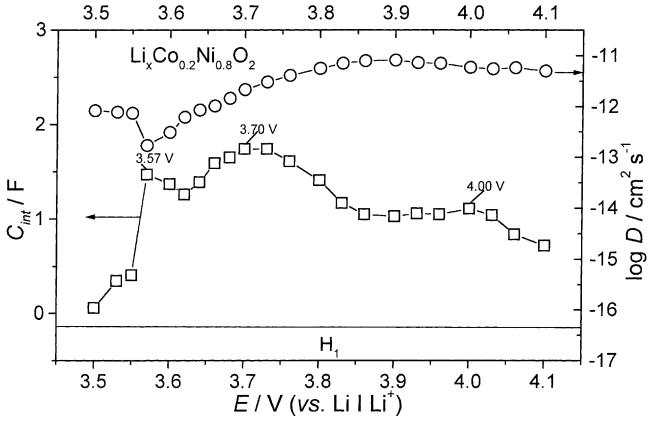

Fig. 2. Plots of the differential intercalation capacity, C_{int} ($v = 10$ μV/s), and the chemical diffusion coefficient of Li-ions, D vs. potential for $Li_xCo_{0.2}Ni_{0.8}O_2$. The phase diagram of this electrode, shown at the bottom, was obtained by XRD [6].

Note that at the bottom of Figs. 1 and 2, we present phase diagrams for both electrodes, indicating single and two-phase co-existence regions (hexagonal, H, and monoclinic, M, phases) obtained by in situ XRD [6]. From these figures, we can conclude that at the beginning of Li-deintercalation, up to $E = 3.62$ V (versus Li/Li^+), similar features are observed for both electrodes: a pronounced minimum in D in the vicinity of $E = 3.57$ V (versus Li/Li^+), corresponding to the maximum in C_{int} around the same potential. An important observation is that within this specific range of potentials both quantities, D and C_{int}, are practically independent of the amplitude of the potential step. Note also that within the same potential range, Li-deintercalation from both electrodes proceeds as a single-phase reaction (hexagonal phase).

In contrast, at higher deintercalation levels, in the range 3.62–4.1 V (versus Li/Li^+), the two electrodes exhibit quite different electroanalytical behavior: sharp peaks on the C_{int} versus E plot for the Li_xNiO_2 electrode, located at 3.66 and 4.04 V (versus Li/Li^+), correlate well with the distinct minima in the log D versus E curve in the vicinity of the same potentials (minor peaks at 3.76 and 3.93 V (versus Li/Li^+) are discussed in [1]). One important feature of these minima was their considerable deepening as the amplitude of the potential increments decreases.

In the case of the $Li_xCo_{0.2}Ni_{0.8}O_2$ electrode for the potential region between 3.62 and 4.15 V (versus Li/Li^+), only two flat peaks at around 3.7 and 4.0 V (versus Li/Li^+) appear in the C_{int} versus E plot. The corresponding log D versus E curve contains only minor features, which were practically independent of the amplitude of the potential steps applied (provided that the potential steps were small enough, in the range of 10 mV).

All the characteristic features related to the shape of D versus E curves for the Li_xNiO_2 and $Li_xCo_{0.2}Ni_{0.8}O_2$

electrodes can be understood in terms of a Frumkin-type intercalation isotherm with short-range interactions between the intercalation species [3,4]. In the limiting case of a quasi-metallic intercalation compound for which the differential intercalation capacity is totally dominated by the availability of Li-sites, both quantities, C_{int} (an equilibrium statistical factor) and D (ion transport factor) can be presented as functions of X (the intercalation level) through one single effective interaction parameter g [4,7]:

$$\frac{C_{int}}{fQ_m} = [g + X^{-1} + (1 - X)^{-1}]^{-1} \quad (3)$$

$$\frac{D}{a_2 k^*} = 1 + g(1 - X)X, \quad (4)$$

where $f = F/RT$ (F and R denote Faraday and gas constants, respectively, and T the absolute temperature); k^* the hopping rate constant [7] for Li-ions, whereas a denotes the separation between nearest insertion sites. One more equation is needed to transform C_{int} versus X curves to C_{int} versus E:

$$E = Q_m \int {C_{int}}^{-1} \, dX + \text{const.} \quad (5)$$

where Q_m is the maximum intercalation charge related to the electrode. Eqs. (1)–(5) provide the necessary basis for the theoretical modeling of both the C_{int} versus E, and D versus E plots as a function of a single interaction parameter g. The results are presented in Fig. 3a and b, respectively (for a detailed discussion see [1]).

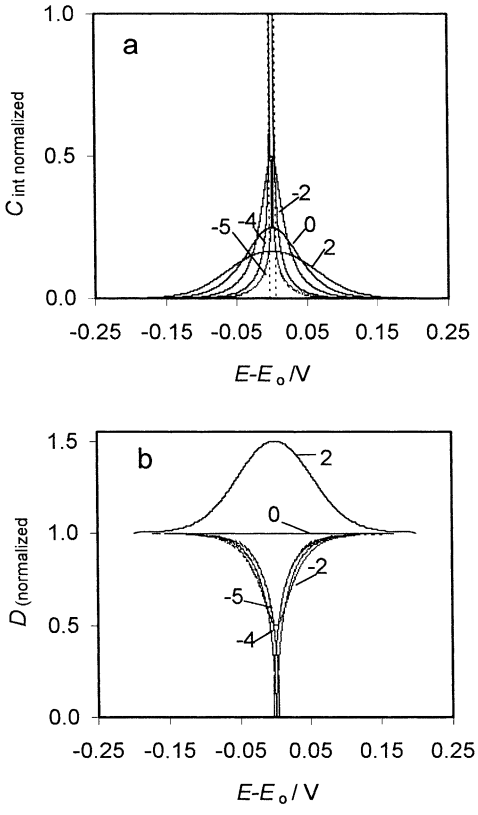

Fig. 3. Plots of theoretical differential intercalation capacity, C_{int} vs. E (a), and theoretical D vs. E (b) calculated from Eqs. (1)–(5) [1].

Depending on the value of g, three different types of the plots, C_{int} and D versus X, are envisaged. A moderate, attractive interaction between the intercalated species ($-4 < g < 0$) results in the appearance of a minimum on the related D versus X curve at $X = 0.5$. This corresponds to a gradual change in X with potential, whereas the bulk of the intercalation electrode presents essentially one single phase. It is understandable that when calculated from PITT, the chemical diffusion coefficient D should be independent of the amplitude of the potential step if the step is sufficiently small (pure equilibrium).

Very high attractive interaction ($g < -4$) leads to a separation between two co-existing phases; D calculated according to this model may be negative for the whole range of X in which two phases co-exist. Obviously, limitations such as retarded Li-ion transfer across surface film/active mass interface, or the slow formation of droplets of a new phase in the bulk of the old one, may conceal the physically unreasonable negative values of D. As a result, small, but positive, values of D are always experimentally obtained. In this case, D calculated from PITT, depends on the amplitude of the applied potential step, exhibiting a more close approach to equilibrium (and hence, a deeper minimum in D) as the amplitude decreases. Finally, repulsive interactions ($g > 0$) result in a maximum on the D versus X curve at $X = 0.5$.

The shape of the C_{int} versus E curve changes correspondingly: as $g > 0$, the half-peak width of the differential capacity curve is larger than 90 mV (for a one-electron reaction). As $g = 0$, the half-peak width takes the Nernstian value 90 mV. Moderate attractive interactions ($-4 < g < 0$) lead to narrow peaks (half-peak width less than 90 mV). Differential capacity curves for very high attractive interactions resulting in first-order phase transition, are described by the so-called δ-function (very sharp peaks).

Thus, in accordance with the above theoretical approach, we ascribe the similar behavior of Li_xNiO_2 and $Li_xCo_{0.2}Ni_{0.8}O_2$ electrodes in the potential region from 3.5 to 3.62 V (versus Li/Li^+) to a moderate attractive interaction between the intercalated species; intercalation proceeds as a single-phase reaction. The differences in the behavior of the two electrodes at higher potentials, between 3.62 and 4.15 V (versus Li/Li^+), are exactly as predicted by the lattice-gas model: for Li_xNiO_2, the inter-site interactions are very high (i.e. negative attraction parameter g), and hence, Li-insertion at potentials higher than 3.62 V (versus Li/Li^+) proceeds via phase transitions. This is well reflected by the sharp minima in C_{int} versus E curves.

4. Conclusion

The electrochemical behavior of Li_xNiO_2 and $Li_xCo_{0.2}Ni_{0.8}O_2$ has been found to correlate strongly with the character of the structural changes occurring in the bulk

of these materials during Li-intercalation and deintercalation. This makes the application of lattice-gas models for the description of Li-intercalation into transition metal oxides both reliable and consistent.

Acknowledgements

Partial support for this study was obtained from the New Energy Development Organization, NEDO, Japan, the German Ministry of Science BMBF, and the DIP program for German-Israeli collaboration, and the National Science Foundation of the Israeli Academy of Science.

References

[1] M.D. Levi, K. Gamolsky, U. Heider, R. Oesten, D. Aurbach, J. Electroanal. Chem. 477 (1999) 32.
[2] D. Aurbach, M.D. Levi, E. Levi, H. Teller, B. Markovsky, G. Salitra, U. Heider, L. Heider, J. Electrochem. Soc. 145 (1998) 3024.
[3] M.D. Levi, G. Salitra, B. Markovsky, H. Teller, D. Aurbach, J. Electrochem. Soc. 146 (1999) 1279.
[4] M.D. Levi, D. Aurbach, Electrochim. Acta 45 (1999) 167.
[5] C.J. Wen, B.A. Boukamp, R.A. Huggins, W. Weppner, J. Electrochem. Soc. 126 (1979) 2258.
[6] E. Levi, M.D. Levi, G. Salitra, D. Aurbach, R. Oesten, U. Heider, L. Heider, Sol. State Ionics 126 (1999) 97.
[7] C.E.D. Chidsey, R.W. Murray, J. Phys. Chem. 90 (1986) 1479.